

SAO LASER REPORT NO. 6

PHOTORECEIVER EFFICIENCY MEASUREMENTS

C. G. Lehr

(NASA-CR-142070) PHOTORECEIVER EFFICIENCY N75-15975
MEASUREMENTS (Smithsonian Astrophysical
Observatory) 41 p HC \$3.75 CSCL 20E
Unclas
G3/36 08988

January 1975



Center for Astrophysics
Harvard College Observatory and Smithsonian Astrophysical Observatory
Cambridge, Massachusetts 02138

TABLE OF CONTENTS

<u>Section</u>		<u>Page</u>
	ABSTRACT	v
1	INTRODUCTION	1
2	QUANTITIES MEASURED	3
3	TECHNIQUE USED	5
4	DESCRIPTION OF THE PHOTORECEIVER	7
5	CALCULATIONS	11
6	PROCEDURE	17
7	COMPUTATIONS	19
8	RESULTS	21
9	ACKNOWLEDGMENTS	25
10	REFERENCES	27
<u>Appendix</u>		
A	BRIGHT STARS USED FOR RECEIVER EFFICIENCY MEASUREMENTS	A-1
B	STATION COORDINATES	B-1
C	FORTH PROGRAM; SAMPLE INPUT AND OUTPUT DATA FOR COMPUTING PMT PARAMETERS	C-1
D	FORTH PROGRAM AND SAMPLE OUTPUT FOR RECEIVER EFFICIENCY COMPUTATIONS	D-1

PRECEDING PAGE BLANK NOT FILMED

ABSTRACT

The efficiency and other related parameters of Smithsonian Astrophysical Observatory's four laser receivers were measured at the observing stations by using equipment already available at the stations. If the efficiency is defined as the number of photoelectrons generated by the photomultiplier tube divided by the number of photons entering the aperture of the receiver, its measured value is about 1% for the laser wavelength of 694 nm. This value is consistent with the efficiency computed from the specified characteristics of the photoreceiver's optical components.

PRECEDING PAGE BLANK NOT FILMED

PHOTORECEIVER EFFICIENCY MEASUREMENTS

C. G. Lehr

1. INTRODUCTION

Laser systems as used for satellite tracking are different from other laser tracking systems (Lehr, 1974). In some ways they are simpler, because:

- A. The objects tracked are in stable orbits.
- B. Output data are not required immediately.

In other ways, they have requirements that are particularly stringent; for example, they must track objects at megameter ranges with decimeter accuracies. Furthermore, the currently shifting emphasis in application from geodesy to geodynamics, along with the launch of spherical satellites such as Lageos and Starlette, will require both increased range and increased accuracy (Kaula, 1969).

Currently, all laser systems for satellite tracking are pulsed systems (Halme, 1973), whose performance is characterized by the amount of energy in the received signal. This energy is low and is usually expressed in photon counts per pulse or, when a photomultiplier tube (PMT) is used, in photoelectrons per pulse. It is important to be able to calculate and measure N , the number of electrons in a return, for two reasons: In the first place, N must be at least unity for the return to be detected, and in the second, the accuracy of a single return increases with N . To see this, consider a pulse of width t ns. Assuming the return has the shape of a normal probability density function, the error associated with a return of a single electron is

$$\sigma_t = \frac{t}{2(2 \ln 2)^{1/2}} \text{ ns} , \quad (1a)$$

This work was supported in part by Grant NGR 09-015-002 from the National Aeronautics and Space Administration.

or

$$\sigma_R = \frac{7.5 t}{(2 \ln 2)^{1/2}} \text{ cm} , \quad (1b)$$

where, for example, $\sigma_R = 127 \text{ cm}$ when $t = 20 \text{ ns}$. However, when $N > 1$, we have

$$\sigma_N = \frac{\sigma_R}{N^{1/2}} , \quad (2)$$

which, for $N = 300$, a value just below the point where PMT saturation begins to set in for the RCA 7265 PMT, is

$$\sigma_N = \frac{127}{300^{1/2}} = 7 \text{ cm} .$$

In calculating and measuring N values, we also determine the laser receiver's efficiency and related quantities. Then we can do the following:

- A. Observe any decrease in receiver efficiency with time.
- B. Compare one laser receiver with another.
- C. Measure atmospheric extinction at the laser wavelength.

2. QUANTITIES MEASURED

The receiver efficiency is the principal result of the measurements described in this report. It is defined herein as the number of photoelectrons generated by the PMT divided by the number of photons reaching the aperture of the receiving telescope. The most important factor in the receiver efficiency is the quantum efficiency of the PMT, but transmission losses in the receiving telescope are also significant. These losses include the aperture blocking of the secondary mirror and its supporting spider, along with absorption in the reflector, lenses, and narrow-band filter. The central wavelength of the measurement is that of the laser, 694 nm, but the measured efficiency is an integrated value over the receiver's bandwidth (several angstroms) rather than over the spectral width ($< 1 \text{ \AA}$) of the transmitted laser energy.

Other quantities are obtained along with the measurement of the receiver's efficiency. Of these, the value of the PMT gain is useful because it influences the noise-figure and gain requirements of the video amplifier that follows the PMT. The single-electron distribution of the PMT is important in distinguishing weak returns from the noise background. The receiver-threshold level can be set lower when this distribution is narrow than when it is wide. The area of a single electron allows the number of electrons in the received pulse to be calculated from the area under the received pulse. The duration of a single-electron pulse is a measure of the overall response time of the receiving system.

3. TECHNIQUE USED

Measuring receiver efficiency is similar to measuring the quantum efficiency of a PMT. A technique commonly used at present for the latter requires a calibrated light source for the input and a discriminator and counter for the gain and output measurement (Klobuchar et al., 1974). The procedure is complicated for the general case because it is necessary to consider the wavelength and intensity of the input light as well as the distribution of the light beam over the photocathode. However, certain simplifications result from the limited nature of the present situation. Our measurements are made only for the ruby-laser wavelength of 694 nm, for intensities below the saturation level of the PMT, and for a light beam that covers the photocathode.

The technique described herein uses only equipment already available at an observing station. The input light flux F and the PMT anode current I_A^* are measured simultaneously. The gain G of the PMT is measured shortly before or after the measurement of F and I_A . The cathode current I is I_A/G . If F is in photons per second and I in electrons per second, the efficiency of the receiver is

$$\eta = \frac{I}{F} \quad (3)$$

Bright stars are used as sources of input light, with values of F computed from tables of narrow-band photometric data. The PMT gain is determined by dividing the average measured output charge of a single-electron pulse by the electronic charge, $q = 1.602 \times 10^{-19}$ Coulomb. The output charge is found by measuring and averaging the areas under single-electron pulses in the anode current. These pulses are displayed on a fast oscilloscope and photographed. The charge, in Coulombs, is the area under one of these pulses when the vertical scale is in amperes and the horizontal scale is in seconds.

* Actually, I_A is the measured anode current less the background current that exists when $F = 0$.

A number of measured pulse areas are averaged to reduce the statistical variation introduced by the dynode amplifiers of the PMT. We use oscilloscope photography because that equipment is already available at the Smithsonian Astrophysical Observatory (SAO) observing stations; there are other less time-consuming possibilities, but they would require additional equipment or modification of components now in use. If a discriminator and frequency counter were available, the cathode current could be measured directly in photoelectrons per second. Or if the "lock-out" feature of the laser system's time-interval counter could be made temporarily inoperative, the cathode current could be obtained by averaging measured intervals between successive electron pulses in the anode current. The cathode current is the reciprocal of this average value.

4. DESCRIPTION OF THE PHOTORECEIVER

A block diagram of the laser receiving system as set up for range measurements (Lehr et al., 1971) is shown in Figure 1. The transmitted and received pulses are displayed on a Tektronix type 454 oscilloscope, whose bandwidth is 150 MHz. Figure 2 is a block diagram for receiver efficiency measurements. The PMT's dc anode current is measured by a microvoltmeter connected across a 100-ohm resistor, and single-electron pulses in the anode current are displayed on the fast oscilloscope. Figure 3 is an optical diagram of the Cassegrain receiving telescope (Gates, 1970), whose characteristics are given in Table 1. A transmission curve for a typical narrow-band filter is reproduced in Figure 4. Pertinent characteristics of the RCA 7265 photomultiplier, taken from the manufacturer's data sheet (RCA, 1968), are listed in Table 2.

Using Tables 1 and 2, we can estimate values to be expected in our measurements. The receiver efficiency should be the quantum efficiency of the PMT times the reflectances of the two mirrors times the transmissions of the three lenses times the transmission of the narrow-band filter, or

$$\eta = 0.025(0.88)^2 (0.999)^3 (0.625) \times 100 = 1.2\% .$$

We can also estimate the background current due to the light from the dark night sky:

$$I_B = N_\lambda \cdot A_R \cdot \Omega_R \cdot \Delta\lambda \cdot \eta \cdot q \cdot G , \quad (4)$$

where

- N_λ = the spectral radiance of the sky,
- A_R = the area of the receiver aperture,
- Ω_R = the field of the receiver (solid angle),
- $\Delta\lambda$ = the bandwidth of the filter,
- η = the receiver efficiency,

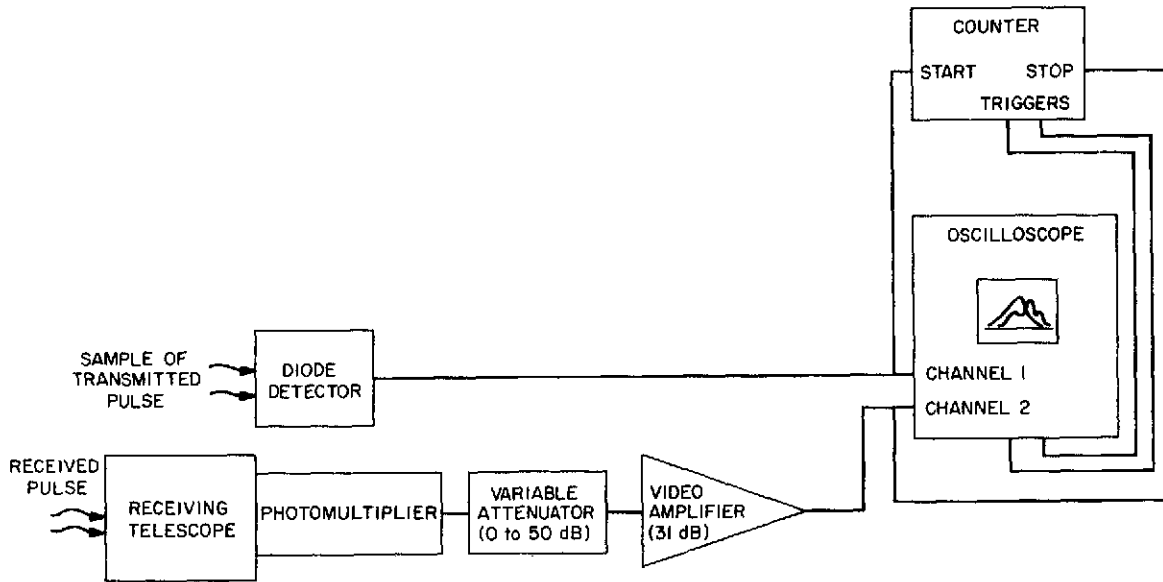


Figure 1. Block diagram for range measurements.

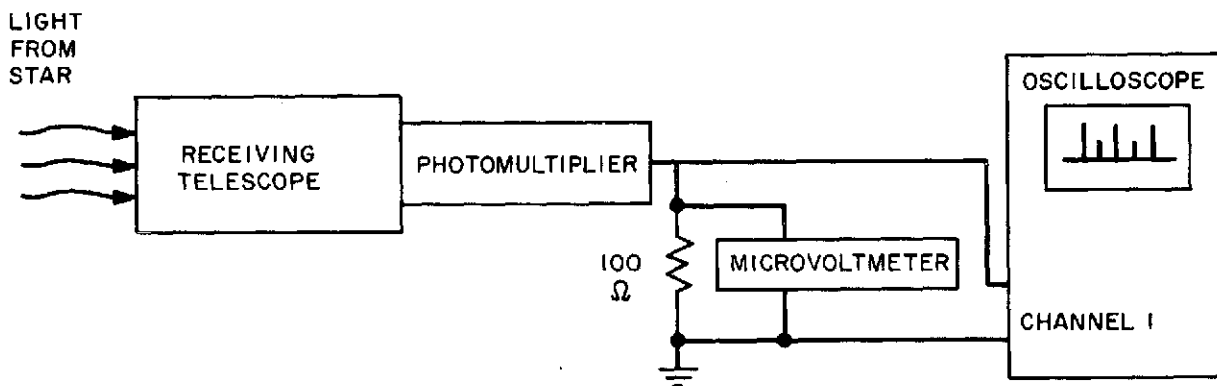


Figure 2. Block diagram for receiver efficiency measurements.

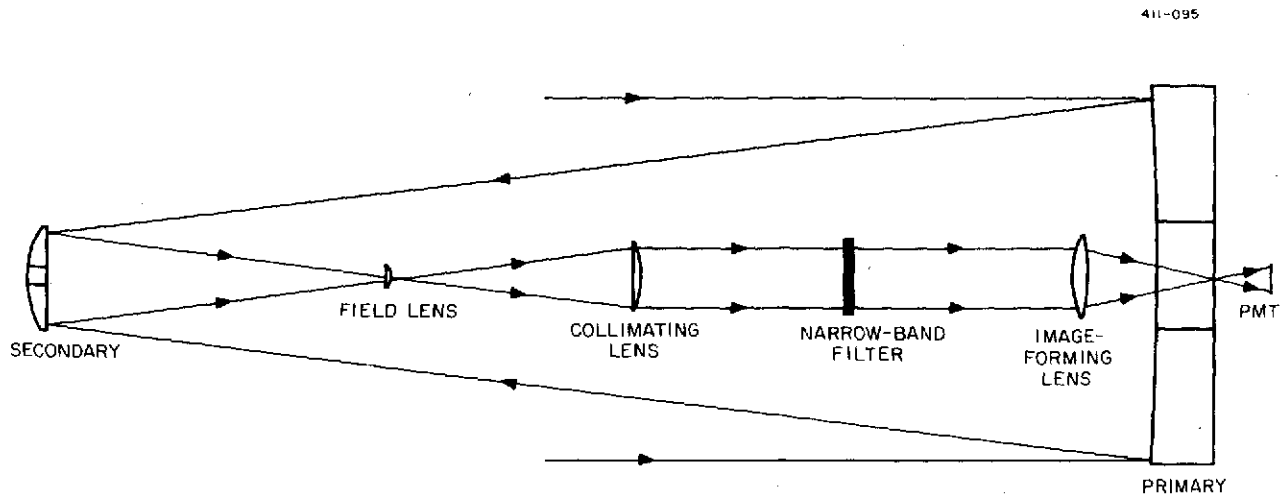


Figure 3. Optical diagram of the photoreceiver.

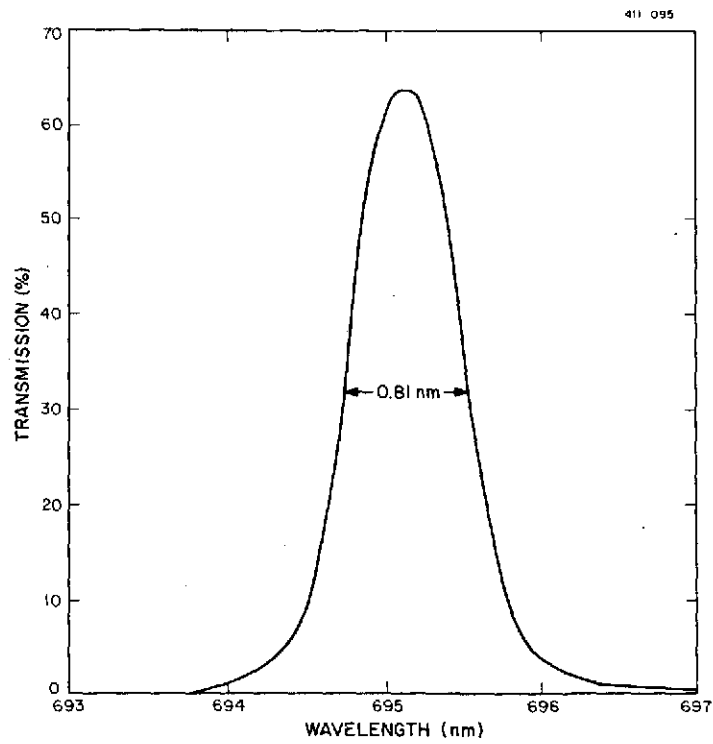


Figure 4. Transmission curve of narrow-band optical filter.

q = the electronic charge,

G = the gain of the PMT.

For the dark night sky, N_λ is approximately 10^{13} photons $s^{-1} m^{-2} sr^{-1} \mu m^{-1}$ (Lehr, 1974; see Table IV). The other quantities are $A_R = 0.2 m^2$, $\Omega_R = 10^{-6} sr$ for a field of 4 arcmin, $\Delta\lambda = 8 \times 10^{-3} \mu m$, $\eta = 1.2\%$, $q = 1.6 \times 10^{-19}$ Coulomb, and $G = 4.8 \times 10^7$. We obtain $I_B = 0.1 nA$, which is negligible compared with the specified dark current of 50 nA. It should be noted, however, that for the most part in our tests, the dark current was only a few nanoamperes.

Table 1. Optical characteristics of the photoreceiver.

<u>Primary Mirror</u>
0.508-m diameter
f/4
parabolic
88% reflectance
<u>Secondary Mirror</u>
0.146-m diameter
flat
88% reflectance
<u>Lenses</u>
99.9% transmission at 694 nm

Table 2. Specified characteristics of the RCA 7265 photomultiplier tube.

Operating voltage	2400 V
Quantum efficiency (at 694 nm)	2.5%
Gain	4.8×10^7
Dark current (at 22°C)	50 nA
Pulse rise time (10 to 90% of peak)	2.7 ns*
Maximum anode current	1 mA

* The equivalent pulse width for a gaussian pulse is 3.8 ns.

5. CALCULATIONS

The first task in calculating the receiver efficiency is to determine F , the input light flux at the laser wavelength. To do so, we must have spectral flux densities for the stars used in the measurements. These are taken from the published results of Mitchell and Johnson (1969) on 1000 bright stars in 13 narrow-wavelength bands. Of use to us is band 72, whose central wavelength is 724 nm and whose effective rectangular bandpass is 8.1% or (695 nm, 753 nm). The ruby-laser wavelength, 694 nm, is at the edge of this band, but adjacent band 63 appears to be less suitable, having a central wavelength of 635 nm and an effective bandwidth of 5.1% or (619 nm, 651 nm).

The stars measured by Mitchell and Johnson are brighter than 5th visual magnitude and north of -20° declination. This declination limit eliminates some bright southern stars (such as Achernar, Antares, Canopus, and Fomalhaut) from the tables. The stars are listed according to their bright-star numbers, found in the Yale Catalog (Hoffleit, 1964). The photometric data are referenced by A0 V stars of zero magnitude. An A0 V star is a main-sequence star whose color index, $B - V$, is zero. Table 2 of Mitchell and Johnson gives an absolute calibration of $1.73 \times 10^{-12} \text{ W cm}^{-2} \mu\text{m}^{-1}$ in filter band 72 for a zero-magnitude A0 V star.

The spectral irradiance of a given star is found by using the absolute calibration from above along with Table 7 of Mitchell and Johnson. This table is entered with the star's bright-star number. Two magnitude values are selected: the one headed 52, which we call x , and the one from the column headed 52-72, which we designate by y . Since x is the magnitude of the star in spectral band 52 and y is the magnitude difference between bands 72 and band 52, we have the following relation:

$$\log_{10} \frac{\ell_0}{\ell} = 0.4 (x - y) \quad , \quad (5)$$

where ℓ_0 and ℓ are, respectively, the spectral irradiance values for the A0 V reference star and for the star in question. Using the given value for ℓ_0 , we have

$$\ell = 1.73 \times 10^{-12} \times 10^{-0.4(x-y)} \text{ W cm}^{-2} \mu\text{m}^{-1} \quad (6a)$$

$$= 6.05 \times 10^{10} \times 10^{-0.4(x-y)} \text{ photons s}^{-1} \text{ m}^{-2} \mu\text{m}^{-1} \quad , \quad (6b)$$

where in equation (6b) we used the fact that $h\nu = 2.86 \times 10^{-19}$ Joule for the laser wavelength, 694 nm. The value of ℓ given by equation (6) is that outside the earth's atmosphere. In computing the light flux entering the aperture of the receiver, we must correct for atmospheric extinction, for which we use

$$T = e^{-\tau/\sin \alpha} \quad . \quad (7)$$

Here, α is the star's altitude angle and τ is given by Kaula (1962), as follows:

$$\tau = \int_{h_0}^{\infty} \left(\frac{0.00114}{\lambda^4} e^{-0.126h} + 0.145 e^{-0.65h} \right) dh \quad , \quad (8)$$

where h_0 is the station height in kilometers and λ is the wavelength in micrometers. The first term in the integrand comes from molecular scattering, with a scale height of 7.9 km. The second term is due to water-vapor absorption, which has a scale height of only 1.5 km and hence is affected significantly by the station's h_0 value. For a ruby laser with $\lambda = 0.694 \mu\text{m}$, equation (8) becomes

$$\tau = 0.0389 e^{-0.126h_0} + 0.223 e^{-0.65h_0} \quad . \quad (9)$$

We can compute α from the epoch of the observation and the coordinates of the star and the station (see Appendices A and B) from the following (Sidgwick, 1971, p. 509):

$$\sin \alpha = \sin \delta \sin \phi + \cos \delta \cos \phi \cos H \quad , \quad (10)$$

where H and δ are the star's hour angle and declination and ϕ is the station's latitude. The hour angle is

$$H = \text{LST} - \text{RA} \quad , \quad (11)$$

where RA is the right ascension of the star and LST, the local sidereal time, is

$$\text{LST} = (1.002738) \text{ UT} + \lambda + \text{ST} \quad , \quad (12)$$

in which UT is the universal time, λ is the east longitude of the station, and ST is the hour angle of the equinox for 0^{h} UT on the day of the measurement. LST, UT, λ , and ST in equation (12) can be expressed in either hours or degrees. The conversion factor is 15° per hour.

We now calculate the input flux F for a given star:

$$F = \ell \cdot A_{\text{R}} \cdot \Delta\lambda \cdot T \text{ photons s}^{-1} \quad , \quad (13)$$

where ℓ and T are given by equations (6b), (7), (9) and (10); $\Delta\lambda$ is the width in micrometers of the narrow-band filter, and A_{R} is the aperture area of the receiving telescope in square meters. The SAO receiving telescope has an aperture diameter of 0.508 m, for which $A_{\text{R}} = 0.203 \text{ m}^2$. The value of $\Delta\lambda$ varies from one filter to another between 7×10^{-4} and $9 \times 10^{-4} \mu\text{m}$. The cathode current I is

$$I = \frac{I_{\text{s}} - I_{\text{b}}}{(1.602 \times 10^{-19})G} \text{ photoelectrons s}^{-1} \quad , \quad (14)$$

where I_{s} is the anode current in amperes with the star in the receiver's field of view, I_{b} is the background current with the star out of the receiver's field, and G is the measured gain of the PMT. At the SAO stations, the PMT output current is measured as a voltage across a 100-ohm resistor. Hence, $I_{\text{s}} = (V_{\text{s}}/100) \times 10^{-6}$ and $I_{\text{b}} = (V_{\text{b}}/100) \times 10^{-6}$, where V_{s} and V_{b} are voltages in microvolts. Equations (3), (13), and (14) give the efficiency of the receiver.

For an idea of the I_{s} values we might expect from various stars, we assume a station at sea level, a star altitude of 45° , a filter bandwidth of 0.7 nm, a receiver

efficiency of 1.2%, and a PMT gain of 4.8×10^7 . For zero background current, we obtain the following expression for I_s from equations (3), (13), and (14):

$$I_s = 9.041 \times 10^{-3} \ell \cdot \mu\text{A} \quad . \quad (15)$$

Estimated I_s values are given in Table 3 for the 18 bright stars selected for the photometric measurements (see Appendix A). The criteria for their selection were as follows:

A. The star must have a name. It was felt that a named star could be easily identified by an observer, who would then check that the proper star was in the field of the telescope.

B. The star must not be variable.

C. The computed PMT current must be $\sim 0.2 \mu\text{A}$ or more so as to be well above the background current.

No attempt was made to track stars during the photometric measurements. The telescope's direction was fixed and the star drifted through. If the telescope's field is f arcmin, the star will be within this field for at least $4f$ s. Hence, for a field of several arcminutes, there is enough time to make the measurement.

Table 3. Characteristics of the 18 stars used for photoreceiver measurements.

Name	Bright- star number	x (52)	y (52-72)	ℓ (photons $s^{-1} m^{-2} \mu m^{-1}$)	Estimated PMT anode current, I_s (μA)
Aldebaran	1457	1.333	1.797	9.269×10^{10}	0.84
Algeiba	4057/8	2.303	1.198	2.185×10^{10}	0.20
Alphard	3748	2.384	1.452	2.563×10^{10}	0.23
Altair	7557	0.799	0.236	3.600×10^{10}	0.32
Arcturus	5340	0.243	1.321	1.632×10^{11}	1.5
Capella	1708	0.243	0.859	1.066×10^{11}	0.96
Deneb	7924	1.309	0.185	2.148×10^{10}	0.19
Dubhe	4301	2.068	1.072	2.416×10^{10}	0.22
Eltanin	6705	2.662	1.675	2.436×10^{10}	0.22
Hamal	617	2.315	1.181	2.128×10^{10}	0.19
Kochab	5563	2.479	1.525	2.511×10^{10}	0.23
Menkar	911	2.951	1.969	2.447×10^{10}	0.22
Mirach	337	2.510	1.873	3.363×10^{10}	0.30
Pollux	2990	1.388	1.025	4.327×10^{10}	0.39
Procyon	2943	0.462	0.485	6.176×10^{10}	0.56
Rigel	1713	0.172	0.080	5.554×10^{10}	0.50
Sirius	2491	-1.421	0.009	2.257×10^{11}	2.0
Vega	7001	0.039	0.008	5.876×10^{10}	0.53

6. PROCEDURE

Receiver efficiency measurements are currently made at least once every 6 months at each of the four observing stations. Before the measurements are started, coordinates in azimuth and altitude for those stars (from Appendix A) that will be more than 20° above the horizon during the period of observation are sent to the station for epochs 5 min apart. Predictions are made for each night over a period of a week to a month by using appropriate subroutines from the satellite-prediction program.

The actual measurements are made on clear nights, and measurements are conducted on several stars, preferably those at high altitudes where the atmospheric correction is minimal. PMT current readings are taken with a high-impedance voltmeter across a 5% 100-ohm resistor that carries the anode of the PMT. The telescope field is set to 4 arcmin, so at least 16 s will be available for the measurement.

The PMT is turned on 10 min before the transit of the first star, and the anode voltage is set to the desired value and measured. The PMT current is read as each star passes through the field, and the background current is read before and after the passage of the star.

Single-electron measurements, needed to find the gain and other relevant parameters of the PMT, are made shortly before or after the star measurements. If desired, an artificial light source can be used. The amount of light entering the PMT is adjusted to give an anode current of $100 \mu\text{A}$, a value that turns out to be convenient for oscilloscope photographs. Expanded pulses, taken with a sweep speed of 5 ns per division (see Figure 5), are used to find the width of a single-electron pulse, and compressed pulses, photographed with a sweep of 200 ns per division, are used to measure the pulse amplitudes. If the gain of the PMT is the specified value, 4.8×10^7 , there should be about 26 compressed pulses on the photograph (see Figure 6). Since the amplitudes have large variations, at least five photographs are taken for a good representation of the distribution.

PRECEDING PAGE BLANK NOT FILMED

One of the uses of the single-electron measurements is to calculate the number of electrons in the return from a satellite or from a fixed reflector on the ground. This number can be obtained from measuring the area under a single-electron pulse. For the SAO systems, the return pulses are displayed after a video amplification of 31 dB, the voltage gain for the Avantek AV-5 amplifier for input signals of 300 mV or less. To take account of video amplification, the pulse areas derived from PMT anode-current measurements are multiplied by $10^{31/20} = 35.5$.

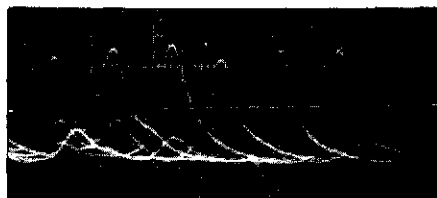


Figure 5. Single-electron pulses: 20 mV per division; 5 ns per division.

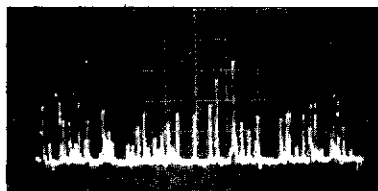


Figure 6. Single-electron pulses: 20 mV per division; 200 ns per division.

7. COMPUTATIONS

Although we have already presented the basic formulas for computing the quantities described in Section 2, a few more details should now be supplied.

The amplitude distribution of single electrons is computed from the measured pulse heights of photographs like Figure 6; the average amplitude is the mean of this distribution. The average pulse width is determined from photographs like Figure 5. The average single-electron area is assumed to be the area under a curve having the shape of a normal distribution with an amplitude equal to the average amplitude and a width equal to the average width. The width of the single-electron pulse is the full width between half-amplitude points. Some pulses, however, are unsymmetrical, having marked changes in slope on their trailing edges, which often occur near the half-amplitude points. For this reason, the pulse width is not measured directly; instead, we measure the area of the pulse and its amplitude. Then the width is taken to be that for a curve having these area and amplitude values and the shape of a normal distribution. If the pulse height is H and the area is A , this width is

$$W = \frac{2A}{H} \left(\frac{\ell n 2}{\pi} \right)^{1/2} = 0.9394 \frac{A}{H} . \quad (16)$$

If W_{av} is the average value of W computed from photographs similar to Figure 5 and H_{av} is the average amplitude from photographs like Figure 6, the average electron area of the pulse before video amplification is

$$A_{av} = \frac{1}{2} \left(\frac{\ell n 2}{\pi} \right)^{-1/2} H_{av} W_{av} . \quad (17)$$

In principle, A_{av} could have been found by averaging the area under several hundred pulses, but in practice, it is not convenient to do so, because many time-consuming area measurements would have to be made. The method actually used takes advantage of the fact that the pulse shape is fairly stable from pulse to pulse, although the pulse amplitudes change markedly.

Two programs were written for the Data General Nova minicomputer in the language Forth (Collins and Cherniack, 1974): the first for computing PMT parameters from single-electron-pulse photographs, and the second for computing receiver efficiency from measurements on the stars. These are given in Appendices C and D.

8. RESULTS

Table 4 summarizes the results of recent photoreceiver measurements at the four SAO stations, and Figure 7 gives plots of single-electron distributions.

The measured values of the efficiency are close to the expected value of 1.2% obtained in Section 4. Errors for the efficiency are sample standard deviations computed from the efficiency values obtained with different stars as references. The single-electron pulse widths are larger than the specified value for the PMT given in Table 2; this stretching may be due to the video circuitry and the oscilloscope that follows the PMT. The PMT gain is consistent with the specified value in Table 2. The broad single-electron distributions shown in Figure 7 are as expected for a tube (such as the RCA 7265) that was not designed to resolve single electrons. Pearl (1967) also found a wide distribution for the RCA 7265.

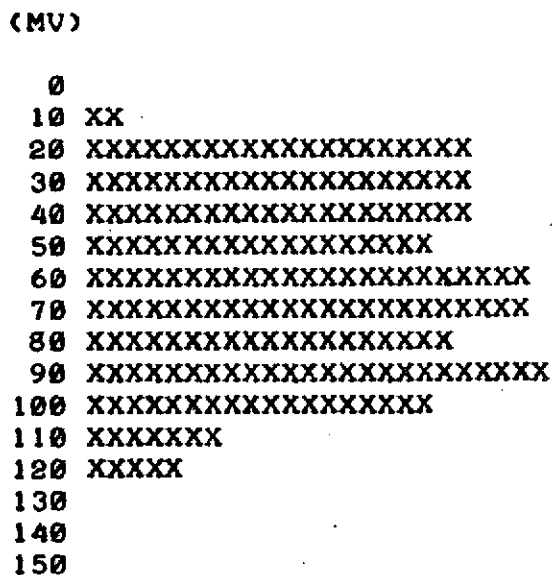


Figure 7. Single-electron distribution. (a) South Africa, July 8, 1974; PMT S24439.

(M.V)

```

0
10 XXXXXXXXXXXXXXXXXXXX
20 XXXXXXXXXXXXXXXXXXXXXXXXXXXXXXXXXXXX
30 XXXXXXXXXXXXXXXXXXXXXXXXXXXXXXXXXXXXXXXXXXXXXXXXXXXXXXXXXXXX
40 XXXXXXXXXXXXXXXXXXXXXXXXXXXXXXXXXXXXXXXXXXXX
50 XXXXXXXXXXXXXXXXXXXXXXXXXXXXXXXXXXXX
60 XXXXXXXXXXXXXXXXXXXXXXXXXXXXXXXXXXXX
70 XXXXXXXXXXXXXXXXXXXXXXXXXXXXXXXXXXXX
80 XXXXXXXXXXXXXXXXXXXXXXXXXXXX
90 XXXXXXXXXXXXXXXXXXXX
100 XXXXXXXXX
110 XXXXXXXX
120 XXXXXXXXXXXXXXXXXXXX
130
140
150

```

Figure 7. Single-electron distribution. (b) Peru, August 1, 1974; PMT S24245.

(MV)

```

0
10 XXXXXXXXXXXXX
20 XXXX
30 XXXXXXXXXXXXXXXXXXXX
40 XXXXXXXXXXXXXXXXXXXX
50 XXXXXXXXXXXXXXXXXXXX
60 XXXXXXXXXXXX
70 XXXXXXXXXXXXX
80 XXXXXXXXXXXXXXXXXXXXXXXXXXXXXXXXXXXXXXXXXXXXXXXXXXXX
90 XXXXXXXXXXXXXXXXXXXX
100 XXXXXXXXXXXXXXXXXXXX
110 XXXXXXXX
120 XX
130 XXXXXXXXXXXXXXXXXXXXXXXXXXXXXXXXXXXXXXXXXXXX
140 XXXXXXXXXXXXXXXXXXXX
150 XXXXXXXXXXXXXXXXXXXX
160 XXXXXXXX
170 XXXXXXXX
180 XXXXXXXXXXXXXXXXXXXXXXXXXXXXXXXXXXXXXXXXXXXX
190 XXXXXXXX
200 XXXX
210 XXXX
220 XXXXXXXX
230 XXXXXXXX
240 XX
250 XX
260 XXXX
270 XX
280 XXXX
290
300 XX
310
320
330
340
350

```

Figure 7. Single-electron distribution. (c) Arizona, July 10, 1974; PMT S24244.

```

(MV)
  0
 10 X
 20
 30 XXXXXXXXXXXXXXXXXXXX
 40 XXXXXXXXXXXXXXXXXXXX
 50 XXXXXXXXXXXXXXXX
 60 XXXXXXXX
 70 XXXXXXXXXXXXXXXXXXXX
 80 XXXXXXXXXXXXXXXXXXXX
 90 XXXXXXXX
100 XXXXXXXXXXXXXXXX
110 XXXXXXXXXXXXXXXXXXXX
120 XX
130 XXXXXXXXXXXXXXXXXXXX
140 XXXXXXXX
150 XX
160 X
170 XXXXX
180 XXXXXXX
190 XX
200 X
210
220
230
240
250 X
260
270
280
290
300
310 X
320
330
340
350

```

Figure 7. Single-electron distribution. (d) Brazil, July 13, 1974; PMT S24240.

Table 4. Results of photoreceiver efficiency measurements at the four SAO stations.

Station	Date of measurement	Receiver efficiency (%)	Average electron amplitude (mV)	Average electron duration (ns)	Area of single electron (V ns)	PMT gain
South Africa	July 8, 1974	1.0 ± 0.2	63	6.5	15.4	5.4×10^7
Peru	Aug. 1, 1974	0.8 ± 0.1	55	5.9	12.2	4.3×10^7
Arizona	July 10, 1974	1.0 ± 0.1	116	6.3	27.5	9.7×10^7
Brazil	July 13, 1974	1.3 ± 0.2	92	7.1	24.6	8.7×10^7

9. ACKNOWLEDGMENTS

I thank Dr. Michael R. Pearlman for his support of this work, which required a commitment of time and manpower at the four stations. I also thank Jakob Wohn and Charles R. H. Tsiang for their helpful advice on many occasions. It is a pleasure to acknowledge the contribution of Jerome R. Cherniack, who patiently taught me Fortran and guided me through the writing of the minicomputer programs. The assistance of the observers at the tracking stations is greatly appreciated; the successful outcome of the measurements depended on their skill and resourcefulness.

10. REFERENCES

- COLLINS, P. L., and CHERNIACK, J. R.
1974. SAO Forth-A primer. Smithsonian Astrophys. Obs., Cambridge, Massachusetts, October, 102 pp.
- GATES, G. M.
1970. Telescope photoreceiver manual. Tinsley Laboratories, Inc., Berkeley, California.
- HALME, S. J.
1973. Workshop on satellite laser systems. Lagonissi 22-25. 5. 1973, Helsinki Univ. Technology, 40 pp.
- HOFFLEIT, D.
1964. Catalogue of Bright Stars. 3rd rev. ed., Yale Univ. Obs., New Haven, Connecticut, 415 pp.
- KAULA, W. M.
1962. Celestial geodesy. Tech. Note, NASA TN D-1155, March, pp. 72-73.
1969. The Terrestrial Environment: Solid-Earth and Ocean Physics (Chairman). Report of a Study at Williamstown, Massachusetts, NASA CR-1579, 147 pp.
- KLOBUCHAR, R. L., AHUMADA, J. J., MICHAEL, J. V., and KAROL, P. J.
1974. An accurate method of photomultiplier gain determination. Rev. Sci. Instr., vol. 45, pp. 1071-1072.
- LEHR, C. G.
1974. Laser tracking systems. In Laser Applications, vol. 2, ed. by M. Ross, Academic Press, New York, pp. 1-52.
- LEHR, C. G., PEARLMAN, M. R., MENDES, G. M., and TSIANG, C. R. H.
1971. The laser network of the Smithsonian Astrophysical Observatory. Presented at the XVth General Assembly of the IUGG, Moscow, August.
- MITCHELL, R. I., and JOHNSON, H. L.
1969. Thirteen-color narrow-band photometry of one thousand bright stars. Comm. No. 132, Lunar Planet. Lab., Univ. Arizona, vol. 8, part 1, 49 pp.

PRECEDING PAGE BLANK NOT FILMED

PEARL, P. R.

1967. Single-electron response of the RCA 7265 photomultiplier. Journ. Sci. Instr., vol. 44, p. 797.

RADIO CORPORATION OF AMERICA

1968. RCA-7265 photomultiplier tube. RCA Electronics Components, Harrison, New Jersey, 8 pp.

SIDGWICK, J. B.

1971. Amateur Astronomer's Handbook. Faber and Faber, London.

APPENDIX A

BRIGHT STARS USED FOR RECEIVER EFFICIENCY MEASUREMENTS*

Name of star	Visual magnitude	Right ascension	Declination
Aldebaran α Tau	1.1	68° 621	+16° 460
Algeiba γ Leo	2.6	154.649	+19.969
Alphard α Hyd	2.2	141.590	- 8.549
Altair α Acq	0.9	297.390	+ 8.801
Arcturus α Boo	0.2	213.630	+19.312
Capella α Aur	0.2	78.710	+45.974
Deneb α Cyg	1.3	310.145	+45.190
Dubhe α UMa	1.9	165.549	+61.886
Eltanin γ Dra	2.4	269.006	+51.491
Hamal α Ari	2.2	31.440	+23.345
Kochab β UMi	2.2	222.690	+74.258
Menkar α Cet	2.8	45.242	+ 3.992
Mirach β And	2.4	17.082	+35.488
Pollux β Gem	1.2	115.947	+28.088
Procyon α CMi	0.5	114.498	+ 5.290
Rigel β Ori	0.3	78.334	- 8.229
Sirius α CMa	-1.6	101.012	-16.681
Vega α Lyr	0.1	279.023	+38.759

* The star positions are for 1975.0 (from The American Ephemeris and Nautical Almanac for the Year 1975, U.S. Govt. Printing Office, Washington, D. C., 1973).

APPENDIX B
STATION COORDINATES*

Station	Height (km)	Latitude	East Longitude
South Africa (7902)	1.544	-25° 959	28° 248
Peru (7907)	2.452	-16.465	288.508
Arizona (7921)	2.383	31.684	249.122
Brazil (7929)	0.046	- 5.928	324.836

* From Gaposchkin, E. M., editor, 1973 Smithsonian Standard Earth (III), Smithsonian Astrophys. Obs. Spec. Rep. No. 353; see especially pp. 339-341.

APPENDIX C

FORTH PROGRAM; SAMPLE INPUT AND OUTPUT DATA
FOR COMPUTING PMT PARAMETERS

Forth Program

```
299
* 45 LOAD START 300 LOAD DONE 1
* ;S
```

```
45
* ( COMPUTATION OF PMT PARAMETERS FROM PULSE HEIGHTS AND WIDTHS ) 1
* DISCARD REMEMBER DISCARD 2
* 3 D ! 3
* ( H-SCALE MV/DIV IS FOR COMPACT PULSES P-SCALE IS FOR PLOT ) 4
* ( W-SCALE NS/DIV IS FOR EXPANDED PULSES ) 5
* ( IN: #BINS, P-SCALE, H-SCALE, W-SCALE ) 6
* ( W: AREA DIV SQ, HEIGHT DIV ) 7
* ( H: HEIGHT DIV ) 8
* 40 LOAD 41 LOAD 42 LOAD 43 LOAD 9
* ;S
```

```
40
* " AVE. ELECTRON AMPLITUDE (MV) = " MESSAGE AVH-M 1
* " X" MESSAGE M 2
* " AVE. ELECTRON DURATION (NS) = " MESSAGE AVW-M 3
* " AREA OF SINGLE ELECTRON (V-NS) = " MESSAGE AREA-M 4
* " PLOT OF SINGLE-ELECTRON DISTRIBUTION: " MESSAGE 5
* PLOT-M 6
* " (MV)" MESSAGE UNITS-M 7
* " PMT GAIN = " MESSAGE GAIN-M 8
* ( CONTINUED ON BLOCK 41 ) 9
* ;S
```

```

41
* 36 INTEGER #BINS I INTEGER P-SCALE 1
* 0. .VAR H-SCALE 0. .VAR W-SCALE 2
* 1 [ 0 #BINS 0 ] ARRAY BIN 3
* 0. .VAR H-SCALE 0. .VAR W-SCALE 4
* 0. .VAR KOUNT 0. .VAR K 0. .VAR Y 5
* 0. .VAR SUM-H 0. .VAR W-SUM 6
* 0. .VAR X 0. .VAR A 0 INTEGER NX 7
* : START CR CR 20 SPACES [ ] BIN MCLEAR 0. KOUNT 0! 8
* 0. K 0! 0. SUM-H 0! 0. W-SUM 0! ; 9
* : PUTINBIN 10. ./ .5 .+ .FIX 1 BIN 10
* DUP @ 1 + SWAP ! ; 11
* ( CONTINUED ON BLOCK 42 ) 12
* ;S

```

```

42
* : IN W-SCALE 0! H-SCALE 0! .FIX P-SCALE ! .FIX #BINS ! ; 1
* : H 0 DO KOUNT 1. .+ KOUNT 0! H-SCALE .* .DUP 2
* PUTINBIN SUM-H .+ SUM-H 0! LOOP ; 3
* : W 2 / 0 DO K 1. .+ K 0! ./ W-SCALE .939437 .* .* 4
* W-SUM .+ W-SUM 0! LOOP ; 5
* : AVH CR CR AVH-M SUM-H KOUNT ./ .DUP 6
* Y 0! .. ; 7
* : AVW CR AVW-M W-SUM K ./ .DUP X 0! .. ; 8
* : AREA CR AREA-M Y X 1.06447 .* .* .DUP 9
* A 0! .035481 .* .. ; 10
* ( CONTINUED ON BLOCK 43 ) 11
* ;S

```

```

43
* : GAIN CR GAIN-M A 50. ./ 1.6021E-7 ./ .. ; 1
* 4 F ! 2
* 0 INTEGER X'S 3
* "XXXXXXXXXXXXXXXXXXXXXXXXXXXXXXXXXXXXXXXXXXXXXXXXXXXXXXXXXXXXXXXXXXXX" 4
* X'S ! 5
* : P X'S @ COUNT DROP NX @ DUP IF TYPE ELSE DROP DROP THEN ; 6
* : PLOT CR CR PLOT-M CR CR UNITS-M CR #BINS @ 7
* 0 DO CR 1 10 * . [ I ] BIN @ P-SCALE @ / 8
* NX ! P LOOP ; 9
* " ELECTRON AMPLITUDES WERE MEASURED" MESSAGE E-M 10
* : ELECTRONS KOUNT .. E-M ; 11
* : DONE AVH AVW AREA GAIN PLOT CR CR ELECTRONS ; 12
* ;S

```


Notes:

- A. # BINS controls the number of 10-mV intervals that will appear in the plot of the single-electron distribution.
- B. H-SCALE (mV/div) and W-SCALE (ns/div) are, respectively, the vertical oscilloscope setting for the compact pulses and the sweep speed for the expanded pulses.
- C. P is a constant that can be increased to prevent the plot of the single-electron distribution from going off scale.

Sample Input Data

300

```
* % PERU 1 AUG 74 PMT S24245 % 1
* 16. 1. 20. 5. IN 2
* [ 2.7 2.4 6.1 4.4 4.6 3.8 4.4 4. 3.2 2. ] W 3
* [ 1.8 1.5 4. 3.3 2.7 2.2 4.6 3.6 5.3 4.4 ] W 4
* [ 2.9 2.2 3.7 2.8 5.9 5. 1.4 1.4 7.5 4.9 ] W 5
* [ 2.7 1.5 4.1 3.1 6. 1.8 2.2 .8 1.5 2.7 ] H 6
* [ 2.4 1.5 3.6 1.6 2. 3.6 2.2 3.6 3.1 1.3 ] H 7
* [ 2.8 1.5 2.4 4.2 4.2 1.4 2.8 1.1 6. 1.7 ] H 8
* [ 1.7 3.2 1.6 2. 2.3 2.5 2.4 5. 4.3 3.3 ] H 9
* [ 3.6 1. 5.8 1.8 1.7 4.1 3.4 .8 1.2 2.6 ] H 10
* [ 3.2 2. 2.5 1.5 2.8 1.4 2.7 4.2 1.5 ] H 11
* [ 1.7 3. 3.4 3.3 5.8 3.4 1.8 6. 2.2 2.4 ] H 12
* [ 1.4 6. 2.4 2.8 1.4 3.1 1.4 .8 4.1 ] H 13
* 301 LOAD 14
* ;S
```

301

```
* [ 6. 2.2 4. 4. 3.1 2.9 .9 5.3 1.7 .6 ] H 1
* [ 3. 1.5 3.1 1.6 1.2 .6 3.4 1. 3. ] H 2
* [ 1.4 1.4 3. 5.6 2.9 3.4 2.1 1.7 1.8 3.4 ] H 3
* [ 1.5 2.9 4.3 1.8 4.8 5.8 2.4 3.8 .9 ] H 4
* [ 1.9 1.6 .4 1. 6. 1.6 3.7 1.8 3.9 3.4 ] H 5
* [ 1.7 5.3 4.1 1.9 4.6 1.9 1.2 4.3 2.3 ] H 6
* [ 1.8 3.7 2.8 2.6 .5 5.1 5.8 1.7 4.5 3.6 ] H 7
* [ 3.5 1.4 3.4 1.5 2. 6. 1.7 2.2 .4 ] H 8
* [ 5.4 1. 3. 2. 4.6 1.7 1.2 .5 4. 1.6 ] H 9
* [ 1.9 3.8 3.4 1.8 3.6 1.6 2.7 6. 4.2 ] H 10
* [ 1. 4.8 3.9 2.4 5.4 2.4 1.4 4.5 1.5 .4 ] H 11
* [ 4.7 1.2 3.7 4.5 3.6 1. 4.3 4. 3.2 ] H 12
* 302 LOAD 13
* ;S
```

302

```
* [ .7 1.2 1.4 1.8 4.7 3.3 2.6 3.4 1.8 4. 4.4 6. ] H 1
* [ 4.2 3. 2.7 3.8 .6 3.4 .7 3.8 1.5 2.5 6. 2.7 ] H 2
* [ 1. .6 4.6 4.5 4.8 3.6 3.7 1.6 3.7 2.7 1.6 .5 ] H 3
* [ 1.2 .7 1. 1.5 2.9 1.9 .6 5.2 1.6 4.2 4. 1. ] H 4
* [ 5.2 1.7 2.3 1.8 5.7 2.8 .5 2.4 3.5 2.6 1.5 .7 ] H 5
* [ 1.9 2.7 3.3 3.3 3. 3.9 4.4 1. 4.4 1.6 3.6 1.7 ] H 6
* [ 3.7 4.6 6. .5 2.3 1.2 1.7 3.4 1.3 4.2 3.2 1.8 ] H 7
* [ 3.4 2.2 2.4 4.6 2. 6. 1.6 .8 1.1 3.6 1.7 1.6 ] H 8
* [ 4.4 2.5 1.2 4.8 .8 2. 2.3 3. 1.1 5.4 2.4 3.8 ] H 9
* [ 1.5 2.1 .5 3.5 1.4 2.7 1.5 ] H 10
* ;S
```

Sample Output Data

299 LOAD

PERU 1 AUG 74 PMT S24245

AVE. ELECTRON AMPLITUDE (MV) = 5.478E+1
AVE. ELECTRON DURATION (NS) = 5.917E+0
AREA OF SINGLE ELECTRON (V-NS) = 1.224E+1
PMT GAIN = 4.307E+7

PLOT OF SINGLE-ELECTRON DISTRIBUTION:

(MV)

```
0
10 XXXXXXXXXXXXXXXXXXXX
20 XXXXXXXXXXXXXXXXXXXX
30 XXXXXXXXXXXXXXXXXXXX
40 XXXXXXXXXXXXXXXXXXXX
50 XXXXXXXXXXXXXXXXXXXX
60 XXXXXXXXXXXXXXXXXXXX
70 XXXXXXXXXXXXXXXXXXXX
80 XXXXXXXXXXXXXXXXXXXX
90 XXXXXXXXXXXXXXXXXXXX
100 XXXXXXXX
110 XXXXXXXX
120 XXXXXXXXXXXXXXXXXXXX
130
140
150
```

3.070E+2 ELECTRON AMPLITUDES WERE MEASURED

APPENDIX D

FORTH PROGRAM AND SAMPLE OUTPUT FOR
RECEIVER EFFICIENCY COMPUTATIONS

Forth Program

```

23
* ( STELLAR PHOTOMETRY )
* DISCARD REMEMBER DISCARD
* 22 LOAD 24 LOAD 25 LOAD 26 LOAD
* 27 LOAD 28 LOAD 29 LOAD 33 LOAD
* 3 D !
* ;S
1
2
3
4
5

22
* " " " MESSAGE M0
* " EFFICIENCY (%) ALTITUDE (DEG) " MESSAGE M1
* " AVERAGE EFFICIENCY (%) = " MESSAGE M2
* " ESTIMATED ERROR =" MESSAGE M3
* : HEADING CR M0 M1 CR ;
* : MA CR CR M2 ;
* : MS CR M3 ;
* ( CONTINUED ON BLOCK 24 )
* ;S
1
2
3
4
5
6
7
8

24
* 0. .VAR FILTER 0. .VAR GAIN 0. .VAR C
* 0. .VAR LAT 0. .VAR LONG
* 0. .VAR L 0. .VAR ST 0. .VAR UT
* 0. .VAR SV 0. .VAR BV 0. .VAR RA
* 0. .VAR DEC 0. .VAR E-S 0. .VAR E-SQ
* 0. .VAR N 0. .VAR E-AV 0. .VAR E
* : ZERO 0. E-S .! 0. E-SQ .! 0. N .! ;
* : DEGREES 3600. ./ .SWAP 60. ./ .+ .+ 15. .* ;
* : RAD 57.2958 ./ ;
* 1 CONSTANT SAFRICA 2 CONSTANT PERU
* 3 CONSTANT ARIZONA 4 CONSTANT BRAZIL
* ( CONTINUED ON BLOCK 25 )
* ;S
1
2
3
4
5
6
7
8
9
10
11
12

```

25

```
* 4 3 MATRIX STATION-ARRAY 1
* : Q 4 1 DO DUP 4 J - 2 STATION-ARRAY .! LOOP DROP ; 2
* .1138 -25.959 28.248 1 Q 3
* .07387 -16.465 288.508 2 Q 4
* .07616 31.684 249.122 3 Q 5
* .2557 -5.928 324.836 4 Q 6
* 1 CONSTANT ALDEBARAN 2 CONSTANT ALGEIBA 7
* 3 CONSTANT ALPHARD 4 CONSTANT ALTAIR 8
* 5 CONSTANT ARCTURUS 6 CONSTANT CAPELLA 9
* 7 CONSTANT DENEK 8 CONSTANT DUBHE 10
* 9 CONSTANT ELTANIN 10 CONSTANT HAMAL 11
* 11 CONSTANT KOCHAB 12 CONSTANT MENKAR 12
* 13 CONSTANT MIRACH 14 CONSTANT POLLUX 13
* 15 CONSTANT PROCYON 16 CONSTANT RIGEL 14
* ( CONTINUED ON BLOCK 26 ) 15
* ;S
```

26

```
* 17 CONSTANT SIRIUS 18 CONSTANT VEGA 1
* 18 3 MATRIX STAR-ARRAY 2
* : R 4 1 DO DUP 4 J - 2 STAR-ARRAY .! LOOP DROP ; 3
* 265.2 68.621 16.460 1 R 4
* 62.52 154.649 19.969 2 R 5
* 73.32 141.590 -8.549 3 R 6
* 103. 297.390 8.801 4 R 7
* 466.9 213.630 19.312 5 R 8
* 305.1 78.710 45.974 6 R 9
* 61.44 310.145 45.190 7 R 10
* 69.13 165.549 61.886 8 R 11
* 69.7 269.006 51.491 9 R 12
* 60.88 31.440 23.345 10 R 13
* ( CONTINUED ON BLOCK 27 ) 14
* ;S
```

```

27
* 71.85 222.690 74.258 11 R 1
* 70.02 45.242 3.992 12 R 2
* 96.22 17.082 35.488 13 R 3
* 123.8 115.947 28.088 14 R 4
* 176.7 114.498 5.290 15 R 5
* 158.9 78.334 -8.229 16 R 6
* 645.7 101.012 -16.681 17 R 7
* 168.1 279.023 38.759 18 R 8
* : STATION GAIN .! FILTER .! [ DUP 1 ] STATION-ARRAY 9
* C .! [ DUP 2 ] STATION-ARRAY LAT .! [ DUP 3 ] 10
* STATION-ARRAY LONG .! DROP HEADING ; 11
* ( CONTINUED ON BLOCK 28 ) 12
* ;S

```

```

28
* : LST UT 1.002738 .* LONG .+ ST .+ ; 1
* : HA LST RA .- ; 2
* : S DEC RAD SIN LAT RAD SIN .* DEC RAD COS 3
* LAT RAD COS HA RAD COS .* .* .+ ; 4
* : A S .DUP .DUP .* .MINUS 1. .+ SQRT ./ ; 5
* : ALTR A ATAN ; 6
* : ALT ALTR 57.2958 .* .. CR ; 7
* : X C .MINUS ALTR SIN ./ ; 8
* ( CONTINUED ON BLOCK 29 ) 9
* ;S

```

```

29
* : ATEN X EXP ; 1
* : CURRENT SV BV .- GAIN ./ 1.6021E-4 ./ ; 2
* : FLUX 7084.5 L FILTER ATEN .* .* .* ; 3
* : KOUNT N 1. .+ N .! ; 4
* : E-SUM E-S E .+ E-S .! ; 5
* : E-SQ-SUM E .DUP .* E-SQ .+ E-SQ .! ; 6
* : AVE KOUNT E-SUM E-SQ-SUM ; 7
* : EFFICIENCY CURRENT FLUX ./ 100. .* .DUP E .! .. AVE ; 8
* : STAR BV .! SV .! DEGREES UT .! DEGREES ST .! 9
* [ DUP 1. ] STAR-ARRAY L .! [ DUP 2 ] STAR-ARRAY 10
* RA .! [ DUP 3 ] STAR-ARRAY DEC .! DROP 11
* EFFICIENCY ALT ; 12
* ( CONTINUED ON BLOCK 33 ) 13
* ;S

```

33

```
* : AV E-S N ./ .DUP E-AV .I .. ; 1
* : STD MS E-AV .DUP .* N .* .MINUS E-SQ .+ 2
* N 1. .- ./ SQRT .. ZERO ; 3
* : TEST N 1. .= IF ZERO ELSE STD THEN ; 4
* : AVERAGE MA AV TEST ; 5
* ;S
```

- Notes:
- A. The 3×4 matrix "station array" contains each station's location (latitude and longitude), along with its constant τ for atmospheric extinction.
 - B. The 18×3 matrix "star array" contains each star's location (right ascension and declination), along with a constant that gives its spectral intensity at 694 nm.

Sample Output

23 LOAD OK

PERU 7. 4.307 STATION

	EFFICIENCY (%)										ALTITUDE (DEG)
HAMAL	20.	32.	56.	07.	15.	02.	17.	1.45	STAR	8.644E-1	3.022E+1
MIRACH	20.	32.	56.	07.	40.	02.	24.	1.50	STAR	7.829E-1	3.289E+1
MENKAR	20.	32.	56.	07.	45.	00.	16.	1.50	STAR	6.889E-1	3.476E+1
ALTAIR	20.	32.	56.	08.	05.	05.	27.	1.55	STAR	8.621E-1	2.463E+1
MIRACH	20.	32.	56.	08.	10.	02.	24.	1.40	STAR	7.796E-1	3.546E+1
MENKAR	20.	32.	56.	08.	15.	01.	18.	1.50	STAR	7.697E-1	4.158E+1
HAMAL	20.	32.	56.	08.	40.	02.	17.	1.50	STAR	8.281E-1	4.363E+1
MENKAR	20.	32.	56.	08.	45.	02.	18.	1.55	STAR	7.581E-1	4.820E+1
HAMAL	20.	32.	56.	09.	10.	02.	18.	1.55	STAR	8.736E-1	4.693E+1
ALDEBARAN	20.	32.	56.	09.	15.	02.	62.	1.60	STAR	7.772E-1	2.846E+1

AVERAGE

AVERAGE EFFICIENCY (%) = 7.985E-1
ESTIMATED ERROR = 5.817E-2

- Notes:
- A. The computation is started by entering the name of the station followed by the bandwidth of the filter (in angstroms), the PMT gain (with the factor 10^{-7} omitted), and the word STATION.
 - B. The photometric observations are entered by the name of the star followed by ST (hours, minutes, seconds) for the date of the observation, UT (hours, minutes, seconds), two readings of the microvoltmeter (with the star in and out of the field), and the word STAR.
 - C. The average efficiency and the estimated error are obtained by entering the word AVERAGE.